# Application of a Hydrogen Storage Alloy with an Amorphous Phase for Sensing Hydrogen in Water

Sumiaki Nakano,* Shin-ichi Yamaura,† Sakae Uchinashi, Hisamichi Kimura,† and Akihisa Inoue†
*Research & Development Center, Home Appliances Manufacturing Division Company, Matsushita Electric Works, Ltd., 1048 Kadoma, Osaka 571-8686*
†*Institute for Materials Research, Tohoku University, 2-1-1 Katahira, Sendai 980-8577*

(Received July 8, 2004; CL-040812)

We investigated the effect of hydrogen on the electrical resistance of melt-spun amorphous alloys. It was found that Mg-based amorphous alloys show the increases in the electrical resistance when they are immersed in hydrogen-dissolved water and that the electrical resistance increases by hydrogen absorption and returns to the initial level by hydrogen desorption. These results show the possibility that the Mg-based amorphous alloys may be applied to hydrogen sensing materials in water.

The catholyte obtained by water electrolysis has been recognized to give good effects for mitigating intestinal and stomach ailments, and hydrogen dissolved in water has been supposed to be one of the factors of the effects.[1] When the effect of hydrogen dissolved in water is clarified, a hydrogen sensor in water will gain more attention. Recently, we have proposed a new type of hydrogen sensor in water, which is made of a hydrogen storage alloy with a single amorphous phase and senses hydrogen by the electrical resistance change accompanied with hydrogen absorption at room temperature in water. In general, compared with crystalline alloys, amorphous ones are known to have more superior properties such as less hydrogen embrittlement, higher strength, and higher corrosion resistance.[2,3] Although there are some gas sensors sensing objects by the electrical resistance change,[4,5] there is none of this type which can sense hydrogen dissolved in water. In order to verify the possibility of our hydrogen sensor in water, the effect of hydrogen on the electrical resistance of melt-spun amorphous alloys was investigated in this work.

From pure metals, ingots of Ni-, Zr-, and Ti-based alloys were prepared with an arc-melting furnace, and those of Mg-based alloys were prepared with a high-frequency induction furnace. From the master alloys, ribbon-shape amorphous alloys of about 0.5 mm width and 15 μm thickness were produced by the single-roller melt-spinning technique. The amorphicity of the melt-spun alloys was examined by X-ray diffractometry (Cu K$\alpha$, 40 kV, 30 mA). Each amorphous sample of 67 mm length was immersed partially, i.e. 47 mm, in pure water of 500 mL, then, the electrical resistance of the alloy was measured with hydrogen bubbling through a glass filter. The hydrogen flow rate was 0.35 mL/s. The hydrogen concentration in water was measured with a hydrogen sensor (TOA DKK, DH METER DH-35A). Electrochemical hydrogen charging and discharging were performed for the $Mg_{87}Al_3Pd_{10}$ amorphous alloy in 6 N KOH solution using a Pt counter electrode and a Ag/AgCl reference electrode. The charging was performed galvanostatically for 300 s at a current density of 24 A/m$^2$. On the other hand, the discharging was performed potentiostatically at $-0.7$ V until the current density decreased to 0.02 A/m$^2$. The potential for the discharging was determined by cyclic voltammetry in 6 N KOH solution.[6] In order to confirm that hydrogen was absorbed and desorbed by the charging and the discharging, differential scanning calorimetry (DSC) was performed for the alloys before and after the charging/discharging at a heating rate of 0.67 K/s. The electrical resistance of the alloy was also measured before and after the charging/discharging.

Figure 1 summarizes the amorphous alloys prepared in this work. Figure 2 shows the X-ray diffraction (XRD) patterns of some of the amorphous alloys. In the XRD pattern of each melt-spun alloy, any distinct crystalline peak is not seen, indicating that each alloy possesses a single amorphous phase. Since the interatomic spacing of an amorphous alloy influences the position of the halo peak in the XRD pattern, Figure 2 suggests, for example, that the structure of the $Ni_{67}Zr_{33}$ amorphous alloy is denser than that of the $Mg_{87}Al_3Pd_{10}$ amorphous alloy.

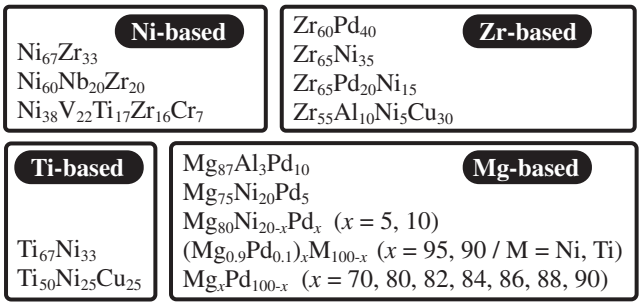


**Figure 1.** List of the amorphous alloys prepared in this work.

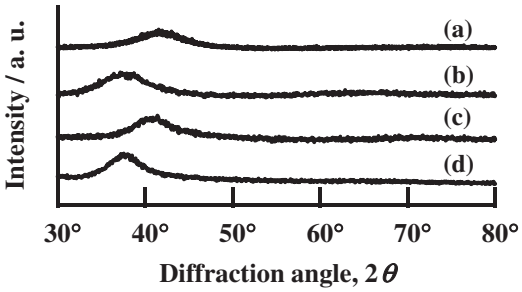


**Figure 2.** XRD patterns of the (a) $Ni_{67}Zr_{33}$, (b) $Zr_{60}Pd_{40}$, (c) $Ti_{67}Ni_{33}$, and (d) $Mg_{87}Al_3Pd_{10}$ amorphous alloys.

When these amorphous alloys are immersed in hydrogen-dissolved water, all the Mg-based amorphous alloys show the increases in the electrical resistance with time, while the Ni-, Zr-, and Ti-based amorphous alloys show no increase. Figure 3 shows the changes in the electrical resistance of Ni-, Zr-, and Ti-based amorphous alloys and some of the Mg-based amor-

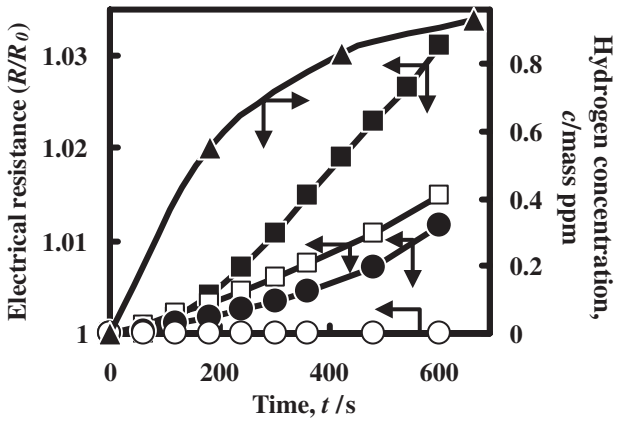


**Figure 3.** Changes in the electrical resistance of the amorphous alloys in hydrogen-dissolved water; ■: $Mg_{80}Ni_{10}Pd_{10}$, □: $Mg_{88}Pd_{12}$, ●: $Mg_{87}Al_3Pd_{10}$, ○: Ni-, Zr-, and Ti-based alloys. The change in the hydrogen concentration (▲) in water is also shown.

phous alloys along with the change in the hydrogen concentration in water. The electrical resistance ($R$) is normalized against the initial one ($R_0$).

In order to confirm the effect of dissolved hydrogen on the electrical resistance of the Mg-based amorphous alloys, we also measured the electrical resistance of the $Mg_{87}Al_3Pd_{10}$ amorphous alloy immersed for 300 s in water with three different hydrogen concentrations of 0.4, 0.9, and 1.1 mass ppm, which reaches the $R/R_0$ values of 1.002, 1.006, and 1.033, respectively. This result suggests that the electrical resistance of the Mg-based amorphous alloys increases more largely in water with higher hydrogen concentration. The effect of hydrogen on the electrical resistance of the $Mg_{87}Al_3Pd_{10}$ amorphous alloy was also investigated by the electrical resistance measurement during the electrochemical hydrogen charging and discharging. Figure 4 shows DSC curves of the $Mg_{87}Al_3Pd_{10}$ amorphous alloy (a) before charging, (b) after charging for 300 s, and (c) after discharging. Three exothermic peaks are seen in curve (a), indicating that the $Mg_{87}Al_3Pd_{10}$ amorphous alloy crystallizes through three stages with the heat treatment. As shown in curve (b), the DSC curve of the hydrogenated sample contains a large endothermic peak due to hydrogen desorption at 380 K which is not seen before the charging. After the discharging, the endothermic peak is not seen in curve (c) and the curve is similar to that before the charging. These results show that the $Mg_{87}Al_3Pd_{10}$ amorphous alloy absorbs and desorbs hydrogen by the charging and the discharging, respectively. Table 1 summarizes the $R/R_0$ values of the $Mg_{87}Al_3Pd_{10}$ amorphous alloys before and after the electrochemical hydrogen charging/discharging. Considering the results of the DSC measurements, it can be said that the electrical resistance increases and decreases by hydrogen absorption and desorption, respectively. This is probably due to the change in the electrical conductivity caused by formation and deformation of hydrides of the amorphous alloy.

The DSC curve of a hydrogenated $Ti_{50}Ni_{25}Cu_{25}$ amorphous alloy, like that of the hydrogenated $Mg_{87}Al_3Pd_{10}$ amorphous alloy, exhibits an endothermic peak due to hydrogen desorption followed by an exothermic peak due to crystallization of the

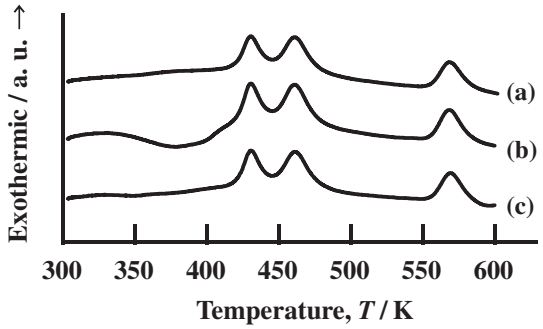


**Figure 4.** DSC curves of the $Mg_{87}Al_3Pd_{10}$ amorphous alloys (a) before charging, (b) after charging for 300 s, and (c) after discharging.

**Table 1.** Electrical resistance of the $Mg_{87}Al_3Pd_{10}$ amorphous alloys (a) before charging, (b) after charging for 300 s, and (c) after discharging

| | (a) | (b) | (c) |
|---|---|---|---|
| $R/R_0$ | 1.00 | 1.16 | 1.00 |

amorphous phase.[7] However, the endothermic peak temperature (500 K) of the hydrogenated $Ti_{50}Ni_{25}Cu_{25}$ amorphous alloy is much higher than that (375 K) of the hydrogenated $Mg_{87}Al_3Pd_{10}$ amorphous alloy. This indicates that hydrogen absorbed in the $Mg_{87}Al_3Pd_{10}$ amorphous alloy is easier to be desorbed than that in the $Ti_{50}Ni_{25}Cu_{25}$ amorphous alloy. In addition, the results of cyclic voltammetry performed in the previous work indicates that the $Mg_{87}Al_3Pd_{10}$ amorphous alloy can absorb and desorb hydrogen more easily than the $Ni_{60}Nb_{20}Zr_{20}$ amorphous alloy.[6] It is conjectured that the mobility of hydrogen in an amorphous alloy influences the hydrogen-sensitivity, and that the interatomic spacing in the amorphous alloy and the formation energy of hydrides are related to the mobility of the hydrogen.

In summary, we have shown that the electrical resistance of the Mg-based amorphous alloys is sensitive to an extremely little hydrogen dissolved in water and that the alloys show good reversibility between the increase and the decrease in the electrical resistance corresponding to hydrogen absorption and desorption. It would appear that hydrogen can be absorbed and desorbed smoothly in the Mg-based amorphous alloys, which leads to the corresponding change in the electrical resistance. The results of this work show the possibility that the Mg-based amorphous alloys may be applied to hydrogen sensing materials in water.

## References

1 K. Kikuchi, *J. Functional Water*, **2**, 65 (2004).
2 A. Inoue, *Mater. Trans.*, **36**, 866 (1995).
3 A. Inoue, *Mater. Sci. Eng.*, **A304–306**, 1 (2001).
4 S. Matsushima, D. Ikeda, K. Kobayashi, and G. Okada, *Chem. Lett.*, **1992**, 323.
5 M. Akiyama, J. Tamaki, N. Miura, and N. Yamazoe, *Chem. Lett.*, **1991**, 1611.
6 S. Nakano, S. Yamaura, S. Uchinashi, H. M. Kimura, and A. Inoue, *Mater. Trans.*, **45**, 2766 (2004).
7 S. Yamaura, M. Hasegawa, H. Kimura, and A. Inoue, *Mater. Trans.*, **43**, 2543 (2002).

Published on the web (Advance View) October 23, 2004; DOI 10.1246/cl.2004.1520